Tracking control strategy for the standard N-trailer mobile robot – geometrically motivated approach

The paper presented during 8^{th} International Workshop RoMoCo 2011, Bukowy Dworek, Poland, June 15-17, 2011

Maciej Michałek
Chair of Control and Systems Engineering
Poznan University of Technology (PUT), Piotrowo 3A, 60-965 Poznań, Poland

Abstract

The paper is devoted to the novel feedback control strategy for the standard N-trailer robot kinematics expected to perform a tracking task for feasible reference trajectories. The control method proposed results from solely geometrical features of vehicle kinematics formulated in a cascaded-form, and especially from the way the velocity components propagate along a vehicle kinematic chain. The control strategy is derived for the original vehicle configuration space not involving any model transformations or approximations. Formal considerations are examined by simulation results of the backward tracking maneuvers for a 3-trailer vehicle.

1 Introduction

Nonholonomic articulated mobile robots consisting of the active tractor linked to the N passive trailers, although fully controllable [8], are especially demanding for control. Difficulties result from three main reasons: the less number of control inputs in comparison to the number of controlled variables in the presence of the nonintegrable motion constraints, the singularities of the vehicle kinematic model [5], and the vehicle folding effect arising during backward maneuvers leading to the so-called jack-knifing phenomenon. The kinematic structure of the N-trailer vehicle can be treated as an equivalent skeleton of many practical vehicles. The manual maneuvers with articulated vehicles are difficult, even for experienced drivers, thus automation of motion control for such vehicles seems to be desirable in practice, [15]. Examples of tracking control laws for the multiple-trailer robots can be found in [2, 10], and for the vehicles with a single trailer in [7, 11]. The most popular approach to the control design relies on the auxiliary transformation of the vehicle model into the chained form, which is possible for the standard N-trailer system due to its differential flatness property, [1, 12–14]. Since the transformation is only locally well defined, utilization of the control solutions based on the chained form approximation may be limiting in applications.

In this paper we present an alternative tracking control strategy for the *standard N-trailer mobile robot* composed of the unicycle-like tractor followed by N passive trailers hooked at a mid-point of a preceding wheel-axle (see Fig. 1). The proposed approach, resulting from geometrical arguments, does not involve any state or input transformations; it is formulated in the original configuration space of the controlled vehicle. The resultant control law has a cascaded structure with clearly interpretable components. As a consequence, tunning of the controller parameters is simple yielding the non-oscillatory vehicle motion in the task space. The concept is formulated using the Vector-Field-Orientation (VFO) control approach for the last vehicle trailer, allowing one to solve the tracking task for the whole set of feasible and persistently exciting reference trajectories (see [4] and also [3]).

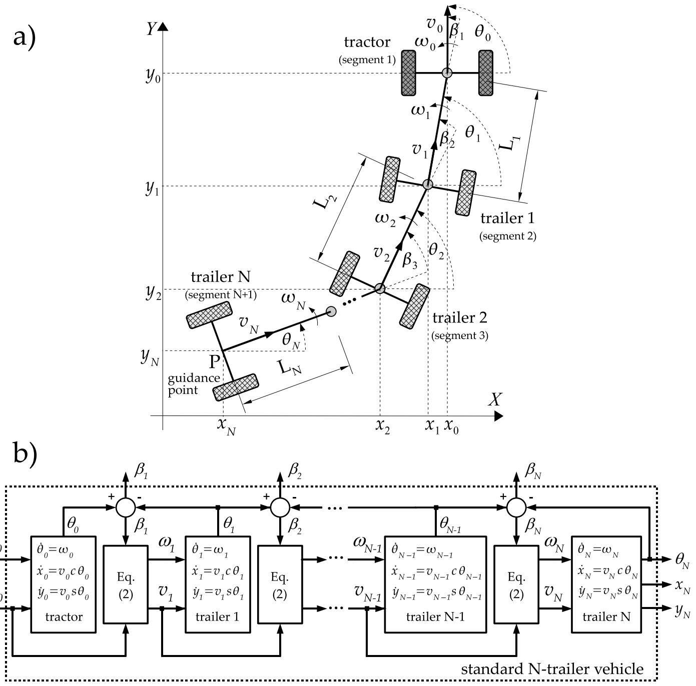

Figure 1: The standard N-trailer vehicle in a global frame (fig. a)) and the schematic diagram of the N-trailer vehicle kinematics in a cascaded form with inputs ω_0, v_0 and configuration $\boldsymbol{q}$ (fig. b)).

2 Vehicle model and the control task

Kinematic skeleton of an articulated vehicle under consideration is presented in Fig. 1. The vehicle consists of $N+1$ segments: the unicycle-like tractor (active segment) followed by N semi-trailers (passive segments) of the length $L_i > 0,\ i = 1, \dots, N$, where every trailer is hitched with a rotary joint located exactly on the axle mid-point of a preceding vehicle segment. Configuration of the vehicle can be represented by vector $\boldsymbol{q} = [\beta_1\ \dots\ \beta_N\ \theta_N\ x_N\ y_N]^T \in \mathbb{R}^{N+3}$ with geometrical interpretation coming from Fig. 1. The *guidance point* $P = (x_N, y_N)$ of the vehicle, playing the key role in the tracking control task (defined in Section 2), is represented by the position coordinates of the last-trailer posture vector $\overline{\boldsymbol{q}} = [\theta_N\ x_N\ y_N]^T \in \mathbb{R}^3$. The control inputs of the vehicle $\boldsymbol{u}_0 = [\omega_0\ v_0]^T \in \mathbb{R}^2$ are the angular ω_0 and the longitudinal v_0 velocities of the tractor.

Let us formulate kinematics of the vehicle in a way useful for the subsequent control development. In order to do this, every i-th segment ($i = 0, 1, \dots, N$) of the vehicle kinematic chain will be described by the unicycle model (cf. Fig. 1):

$$\dot{\theta}_i = \omega_i, \qquad \dot{x}_i = v_i \cos\theta_i, \qquad \dot{y}_i = v_i \sin\theta_i. \tag{1}$$

The tractor kinematics is obtained taking $i = 0$ where ω_0 and v_0 are the physical control inputs. For $i = 1, 2, \dots, N$ the fictitious control inputs ω_i, v_i of the i-th trailer result from two recurrent equations:

$$\omega_i = \frac{1}{L_i} v_{i-1} \sin\beta_i, \qquad v_i = v_{i-1} \cos\beta_i, \tag{2}$$

where β_i is the i-th joint angle determined by

$$\beta_i = \theta_{i-1} - \theta_i. \tag{3}$$

Using equations (2)-(3) one can describe how the physical inputs ω_0 and v_0 propagate to the i-th trailer along the vehicle kinematic chain. This is explained by the block diagram in Fig. 1 (subfigure b)), which represents the general N-trailer vehicle kinematics in the above cascaded-like formulation [12].

Since the guidance point $P = (x_N, y_N)$ has been selected on the last trailer, the control task will be formulated with a special attention paid to the last vehicle segment. This selection of the guidance point is theoretically justified, since the coordinates x_N, y_N are the *flat outputs* of the vehicle kinematics [13], and the differential flatness is a key feature implicitly utilized in the subsequent control development.

Let $\boldsymbol{q}_t(\tau) = [\beta_{t1}(\tau) \ \dots \ \beta_{tN}(\tau) \ \theta_{tN}(\tau) \ x_{tN}(\tau) \ y_{tN}(\tau)]^T \in \mathbb{R}^{N+3}$ denote the reference configuration trajectory of the vehicle. Define the configuration tracking error $\boldsymbol{e}(\tau) = \left[\boldsymbol{e}_\beta^T(\tau) \ \overline{\boldsymbol{e}}^T(\tau)\right]^T \triangleq \boldsymbol{q}_t(\tau) - \boldsymbol{q}(\tau)$ with the joint-angle tracking error component

$$\boldsymbol{e}_\beta(\tau) \triangleq [\beta_{t1}(\tau) - \beta_1(\tau) \ \dots \ \beta_{tN}(\tau) - \beta_N(\tau)]^T \in \mathbb{R}^N \tag{4}$$

and the last-trailer posture tracking error component

$$\overline{\boldsymbol{e}}(\tau) = \begin{bmatrix} e_\theta \\ e_x \\ e_y \end{bmatrix} \triangleq \overline{\boldsymbol{q}}_t(\tau) - \overline{\boldsymbol{q}}(\tau) = \begin{bmatrix} \theta_{tN}(\tau) - \theta_N(\tau) \\ x_{tN}(\tau) - x_N(\tau) \\ y_{tN}(\tau) - y_N(\tau) \end{bmatrix} \in \mathbb{R}^3. \tag{5}$$

Assuming that:

- A1 the reference trajectory $\boldsymbol{q}_t(\tau)$ is feasible (meets the vehicle kinematics for all $\tau \geqslant 0$) and is persistently exciting, namely $\dot{x}_{tN}^2(\tau) + \dot{y}_{tN}^2(\tau) \neq 0$ for all $\tau \geqslant 0$,
- A2 all components of the configuration $\boldsymbol{q}$ are measurable,
- A3 all the vehicle kinematic parameters L_i are known,

the control problem is to design a feedback control law $\boldsymbol{u}_0 = \boldsymbol{u}_0(\boldsymbol{q}_t(\tau), \boldsymbol{q}(\tau), \cdot)$ which applied to the vehicle kinematics represented by (1)-(3) makes the error $\boldsymbol{e}(\tau)$ convergent in the sense that:

$$\lim_{\tau\to\infty} \|\,\overline{\boldsymbol{e}}(\tau)\| \leqslant \delta_1 \quad \text{and} \quad \lim_{\tau\to\infty} \|\,\boldsymbol{e}_\beta(\tau)\| \leqslant \delta_2, \tag{6}$$

with τ denoting the time variable, and $\delta_1, \delta_2 \geqslant 0$ are the vicinities of zero in the particular tracking error spaces. In the paper the two cases of asymptotic ($\delta_1 = \delta_2 = 0$) and *practical* ($\delta_1, \delta_2 > 0$) convergence will be illustrated.

3 Feedback control strategy

The proposed control strategy for the standard N-trailer robot results from equations (2) which describe propagation of the tractor velocities to particular trailers along the vehicle kinematic chain. In order to explain our concept let us begin from the last vehicle trailer where the guidance point P is located. We can make a thought experiment where the N-th trailer is separated from the remaining vehicle chain and treated as the unicycle-like vehicle with control inputs ω_N, v_N (cf. Fig. 1). Furthermore, let us assume that feedback control functions $\omega_N := \Phi_\omega(\overline{\boldsymbol{e}}(\tau), \cdot)$ and $v_N := \Phi_v(\overline{\boldsymbol{e}}(\tau), \cdot)$ (defined in Section 3.2) which ensure asymptotic convergence of the tracking posture error $\overline{\boldsymbol{e}}(\tau)$ for the unicycle model (1) with $i := N$ are given.

Formulating the control strategy we need to answer the question: how can one force the control signals $\omega_N := \Phi_\omega$ and $v_N := \Phi_v$ in the case when the N-th trailer is not driven directly, but it is passive and linked to the whole kinematic chain driven only by the tractor inputs ω_0, v_0. One can answer the question utilizing the fact that the motion of the N-th trailer is a direct consequence of motion of the $(N-1)$-st trailer. Thus designing the appropriate desired motion for the latter can help forcing the desired control action determined by functions Φ_ω and Φ_v for the N-th trailer. Relations (2) reveal how to design the fictitious input v_{N-1} of the $(N-1)$-th trailer and the joint angle β_N and, as a consequence, the design of the fictitious input ω_{N-1} can be devised (it will be formalized in the next subsection). Again, the fictitious inputs v_{N-1}, ω_{N-1} cannot be forced directly, but only through the $(N-2)$-nd vehicle segment. Proceeding analogous reasoning for the whole kinematic chain (where the i-th segment influences motion of the $(i+1)$-st), one can derive the control law for physically available tractor inputs ω_0, v_0, which should accomplish the desired motion of the last trailer (*guiding* segment).

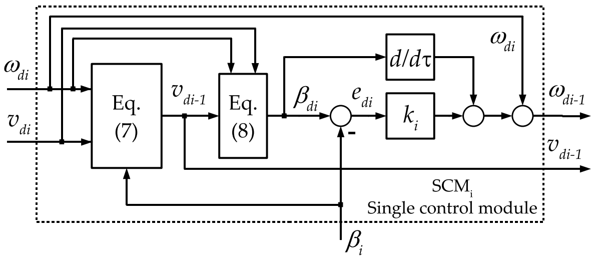

Figure 2: Schema of the i-th Single Control Module (SCM$_i$) with a feedback from joint angle β_i.

3.1 Control law design

Denote by ω_{di} and v_{di} $(i = 1, \ldots, N)$ the desired fictitious inputs which the i-th vehicle segment should be forced with in order to execute the desired motion of the $(i+1)$-st segment. Formulas which determine the desired longitudinal velocity v_{di-1} for the $(i-1)$-st vehicle segment and the desired value for the i-th joint angle can be obtained by combination of relations (2), namely:

$$v_{di-1} \triangleq L_i \omega_{di} \sin\beta_i + v_{di} \cos\beta_i, \tag{7}$$

$$\beta_{di} \triangleq \operatorname{Atan2c}\left(L_i\omega_{di} \cdot v_{di-1}, v_{di} \cdot v_{di-1}\right) \in \mathbb{R}, \tag{8}$$

where $\operatorname{Atan2c}(\cdot,\cdot) : \mathbb{R} \times \mathbb{R} \mapsto \mathbb{R}$ is a continuous version of the four-quadrant function $\operatorname{Atan2}(\cdot,\cdot) : \mathbb{R} \times \mathbb{R} \mapsto (-\pi, \pi]$ (it has been introduced to ensure continuity of β_{di} signals[1]), and the term v_{di-1} used in (8) determines the appropriate sign of the two function arguments. Whereas equation (7) determines one of the desired fictitious inputs of the $(i-1)$-st segment, the desired angular fictitious input ω_{di-1} remains to be determined. To do this let us differentiate relation (3) and utilize (1) to obtain

$$\dot{\beta}_i = \omega_{i-1} - \omega_i =: \nu_i. \tag{9}$$

The above relation may suggest definition of ν_i to make the auxiliary joint angle error

$$e_{di} \triangleq (\beta_{di} - \beta_i) \in \mathbb{R} \tag{10}$$

converge to zero. By taking $\nu_i \triangleq k_i e_{di} + \dot{\beta}_{di}$ with $k_i > 0$ and $\dot{\beta}_{di} \equiv d\beta_{di}/d\tau$, one gets the differential equation $\dot{e}_{di} + k_i e_{di} = 0$, which implies the exponential convergence $e_{di}(\tau) \to 0$ as $\tau \to \infty$. According to (9), the desired angular velocity for the $(i-1)$-st vehicle segment can be defined as follows:

$$\omega_{di-1} \triangleq \nu_i + \omega_{di} \triangleq k_i e_{di} + \dot{\beta}_{di} + \omega_{di}, \tag{11}$$

where $k_i > 0$ is now a control design coefficient, and $\dot{\beta}_{di}$ plays a role of the feed-forward component.

Definitions (7), (8), and (11) constitute the so-called i-th Single Control Module (SCM$_i$) explained by the schematic diagram in Fig. 2, where the feedback from the joint angle β_i has been denoted. Serial connection of SCM$_i$ blocks allows propagating the computations of desired velocities between arbitrary number of vehicle segments. Recurrent relations formulated in (7), (8), and (11) are iterated from $i = N$ to $i = 1$, starting from the last trailer by taking $\omega_{dN} := \Phi_\omega(\overline{\boldsymbol{e}}(\tau), \cdot)$, $v_{dN} := \Phi_v(\overline{\boldsymbol{e}}(\tau), \cdot)$ and finishing on the tractor segment obtaining the control inputs $\omega_0 := \omega_{d0}(\cdot)$, $v_0 := v_{d0}(\cdot)$. Equations of the resultant feedback controller for the standard N-trailer

[1]We refer to [4] for computation details of $\operatorname{Atan2c}(\cdot,\cdot)$ function.

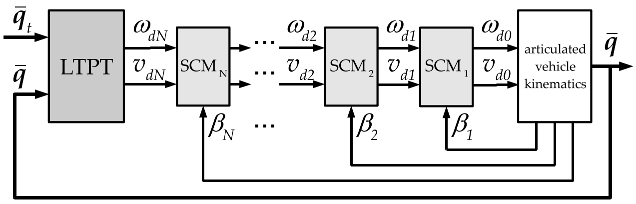

Figure 3: Schema of the proposed cascaded control system for the standard N-trailer vehicle. The controller consists of N Single Control Modules using a feedback from joint angles β_i, and the Last-Trailer Posture Tracker (LTPT) block designed for the last trailer treated as the unicycle.

vehicle are formulated as follows:

$$v_{dN} := \Phi_v(\overline{\boldsymbol{e}}(\tau), \cdot) \tag{12}$$
$$\omega_{dN} := \Phi_\omega(\overline{\boldsymbol{e}}(\tau), \cdot) \tag{13}$$
$$v_{dN-1} := L_N \omega_{dN} \sin\beta_N + v_{dN}\cos\beta_N \tag{14}$$
$$\beta_{dN} := \text{Atan2c}\left(L_N\omega_{dN}\cdot v_{dN-1}, v_{dN}\cdot v_{dN-1}\right) \tag{15}$$
$$\omega_{dN-1} := k_N(\beta_{dN} - \beta_N) + \dot{\beta}_{dN} + \omega_{dN} \tag{16}$$
$$\vdots$$
$$v_{d1} := L_2\omega_{d2}\sin\beta_2 + v_{d2}\cos\beta_2 \tag{17}$$
$$\beta_{d2} := \text{Atan2c}\left(L_2\omega_{d2}\cdot v_{d1}, v_{d2}\cdot v_{d1}\right) \tag{18}$$
$$\omega_{d1} := k_2(\beta_{d2} - \beta_2) + \dot{\beta}_{d2} + \omega_{d2} \tag{19}$$
$$v_0 = v_{0d} := L_1\omega_{d1}\sin\beta_1 + v_{d1}\cos\beta_1 \tag{20}$$
$$\beta_{d1} := \text{Atan2c}\left(L_1\omega_{d1}\cdot v_{d0}, v_{d1}\cdot v_{d0}\right) \tag{21}$$
$$\omega_0 = \omega_{d0} := k_1(\beta_{d1} - \beta_1) + \dot{\beta}_{d1} + \omega_{d1}. \tag{22}$$

Equations (20) and (22) express direct application of the desired velocities computed for the vehicle segment number zero to the control inputs of the vehicle tractor. Figure 3 illustrates the structure of the proposed cascaded control system, where the Last-Trailer Posture Tracker (LTPT) block represents the tracking control module designed for the unicycle kinematics of the last trailer. This block computes the feedback control functions $\Phi_\omega(\overline{\boldsymbol{e}}(\tau), \cdot)$ and $\Phi_v(\overline{\boldsymbol{e}}(\tau), \cdot)$ used in equations (12)-(13). Note that according to the defined control task (cf. Section 2) the controlled output of the articulated vehicle is the last trailer posture $\overline{\boldsymbol{q}} \in \mathbb{R}^3$, while the angles β_1 to β_N are the auxiliary outputs used in the SCM$_i$ blocks.

Control strategy presented so far generally does not prevent the vehicle folding effect. It is a consequence of definition (8), where the desired angles are the real (unbounded) variables. Since it may be limiting in most practical application, we propose to modify definition (7) in order to avoid the folding effect by taking:

$$v_{di-1} \triangleq \sigma \left| L_i\omega_{di}\sin\beta_i + v_{di}\cos\beta_i \right|, \tag{23}$$

where $\sigma \in \{-1, +1\}$ is the decision variable which is inherited from the VFO controller used in LTPT block and determined in Subsection 3.2. By modification (23) and leaving other definitions unchanged, and due to characteristic features of the VFO controller (see [4]) the second argument of Atan2c $(\cdot,\cdot)$ function in (8) may now have a constant non-negative sign for almost all time of the vehicle motion. Hence, the image of function Atan2c $(\cdot,\cdot)$ can be limited to the first and fourth quadrant, minimizing possibility of the folding effect occurence. Summarizing, the only modifications of the controller (12)-(22) are required for (14), (17), and (20) by replacing them with definition (23) using the appropriate indexes.

To accomplish derivation of a feedback controller for the articulated vehicle it remains to determine the feedback functions Φ_v and Φ_ω used by the LTPT block (see (12)-(13)). Explicit definitions of these functions are given and briefly commented in the next subsection using the original VFO concept.

3.2 Last-Trailer Posture Tracker – the VFO controller

The VFO control approach comes from geometrical interpretations related to the unicycle kinematics (1). Our selection of the VFO method for the LTPT block is motivated by the specific features of the VFO controller, which guarantees fast and non-oscillatory tracking error convergence in the closed-loop system. Let us briefly recall equations of the VFO tracker, written for the unicycle model of the last trailer, with short explanation of its particular terms (more detailed description can be found in [4]).

The VFO controller can be formulated as follows:

$$\Phi_\omega \triangleq k_a e_a + \dot{\theta}_a, \qquad \Phi_v \triangleq h_x \cos\theta_N + h_y \sin\theta_N, \tag{24}$$

where Φ_ω is called the *orienting control*, and Φ_v the *pushing control*. Particular terms in the above definitions are determined as follows:

$$h_x = k_p e_x + \dot{x}_{tN}, \qquad h_y = k_p e_y + \dot{y}_{tN}, \qquad e_a = \theta_a - \theta_N, \tag{25}$$

$$\theta_a = \mathrm{Atan2c}\left(\sigma \cdot h_y, \sigma \cdot h_x\right), \qquad \dot{\theta}_a = (\dot{h}_y h_x - h_y \dot{h}_x)/(h_x^2 + h_y^2), \tag{26}$$

where $k_a, k_p > 0$ are the design coefficients. The decision factor $\sigma \triangleq \mathrm{sgn}(v_{tN}) \in \{-1, +1\}$ (used also in (23)) allows designer to select the desired motion strategy: forward if $v_{tN}(\tau) > 0$ or backward if $v_{tN}(\tau) < 0$, where $v_{tN}(\tau) = \sigma\sqrt{\dot{x}_{tN}^2(\tau) + \dot{y}_{tN}^2(\tau)}$ denotes the reference longitudinal velocity defined along $\overline{\boldsymbol{q}}_t(\tau)$. Note that e_x and e_y are the components of error (5). It has been proved in [4] that functions defined by (24) guarantee asymptotic convergence of error $\overline{\boldsymbol{e}}(\tau)$ to zero assuming that they are directly forced as inputs to the unicycle-like kinematics.

In the case of an articulated vehicle the functions (24) have to be substituted into (12) and (13) yielding the complete tracking controller for the N-trailer vehicle.

Remark 1 *The desired joint angles (8) and their time-derivatives are undetermined at the time instants τ_I when the two arguments of function Atan2c$(\cdot,\cdot)$ are simultaneously equal to zero. We propose to cope with this problem using at τ_I the limit values β_{di}^- and $\dot{\beta}_{di}^-$, where $\beta_{di}^- = \lim_{\tau\to\tau_I^-}\beta_{di}(\tau)$ and $\dot{\beta}_{di}^- = \lim_{\tau\to\tau_I^-}\dot{\beta}_{di}(\tau)$.*
The explicit formulas of time-derivatives $\dot{\beta}_{di}$ used in eqs. (16), (19), and (22) may be obtained by formal differentiation of definition (8), which involves the time-derivatives of signals ω_{di} and v_{di}. Since this may cause difficulties in practical implementation, we propose to use instead the so-called robust exact differentiator *proposed in [9], or approximate the terms $\dot{\beta}_{di}$ by their filtered versions $\dot{\beta}_{diF} = \mathcal{L}^{-1}\{s\beta_{di}(s)/(1 + sT_F)\}$, which are numerically computable. For tracking the rectilinear or circular reference trajectories the terms $\dot{\beta}_{di}$ can be even omitted in control implementation (since now $\dot{\beta}_{ti} \equiv 0$), assuming however sufficiently high values for gains k_i to preserve stability of the closed-loop system. Control effectiveness in the latter case will be illustrated by simulation Sim2 in the next section.*

4 Simulation results and discussion

Performance of the closed-loop system with the proposed tracking controller is illustrated by the results of two simulations of backward motion maneuvers: for the *advanced* reference trajectory (Sim1), and for the circular reference trajectory (Sim2). The reference signals $\overline{\boldsymbol{q}}_t(\tau)$ have been generated as a solution of the unicycle model with the reference inputs $\omega_{t3} := 0.15(1+\sin 0.3\tau)$ rad/s, $v_{t3} := -0.2$ m/s for Sim1, and $\omega_{t3} := 0.15$ rad/s, $v_{t3} := -0.2$ m/s for Sim2, taking the initial configuration for the reference vehicle $\boldsymbol{q}_t(0) = [0\ 0\ 0\ \frac{\pi}{2}\ {-1}\ 0]^T$. Vehicle initial configurations have been selected as follows: $\boldsymbol{q}(0) = [0\ 0\ 0\ \frac{\pi}{2}\ 0\ 0]^T$ for Sim1, and $\boldsymbol{q}_t(0) = [0\ 0\ 0\ \pi\ 0\ 0]^T$ for Sim2. The following common numerical values have been selected for both simulations: $L_1 = L_2 = L_3 = 0.25$ m, $k_1 = 50$, $k_2 = 20$, $k_3 = 5$, $k_a = 2$, $k_p = 1$. For Sim1 the feed-forward terms $\dot{\beta}_{di},\ i = 1, 2, 3$ have been approximated by $\dot{\beta}_{diF}$ (see Remark 1) using the filter time-constant $T_F = 0.05$ s. In the case Sim2, the simplified control implementation with $\dot{\beta}_{d2,3} := 0$ has been used. The results of simulations are presented in Fig. 4. For the two simulation tests the relatively demanding initial configurations of the controlled vehicle have been selected in order to show effectiveness of the proposed control strategy, especially in the context of the vehicle folding effect avoidance.

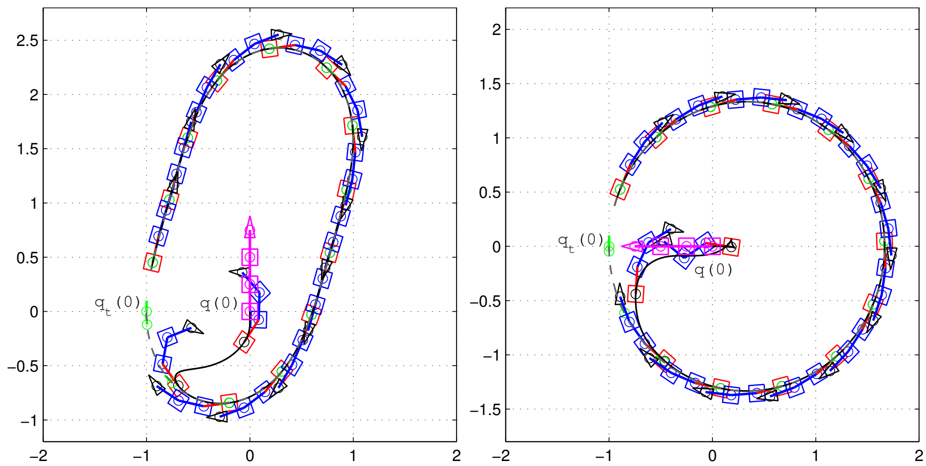

Figure 4: Backward tracking maneuvers in the (x, y) plane (dimensions in [m]): for the advanced reference trajectory (Sim1, left) and for the circular trajectory (Sim2, right). Initial vehicle configuration $\boldsymbol{q}(0)$ and initial reference configuration $\boldsymbol{q}_t(0)$ are denoted in the figure (the former is highlighted in magenta); the last trailer is denoted by the red rectangle, the tractor – by the black triangle; evolution of the reference trailer posture is denoted by the green marks.

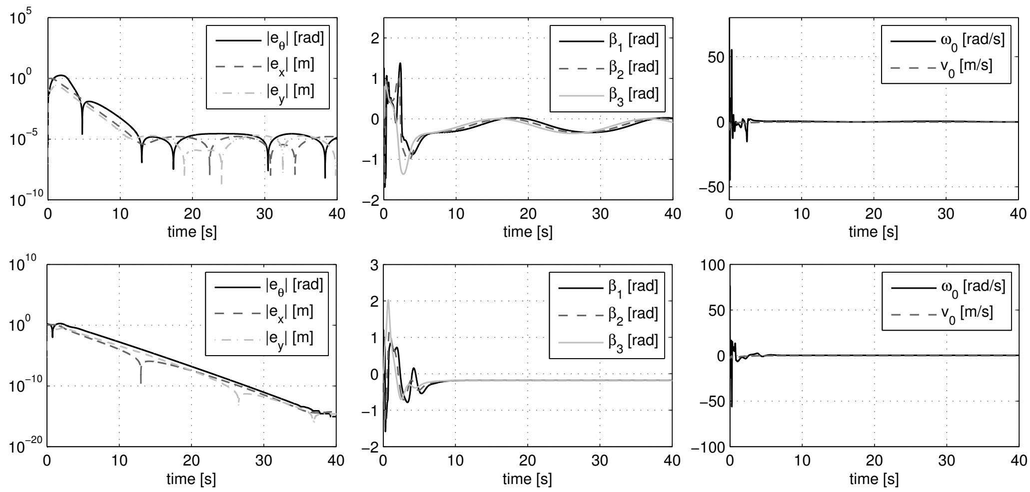

Figure 5: Time plots of the last-trailer posture errors in a logarithmic scale (left), the vehicle joint angles (middle), and the tractor control inputs (right) for simulation Sim1 (top) and Sim2 (bottom).

Reference trajectories selected for simulations Sim1 and Sim2 differ each other qualitatively. For the circular trajectory (Sim2) the reference velocities and reference joint angles remain constant, while for the *advanced* trajectory they are time-varying (it justifies the term *advanced trajectory* for Sim1). Tracking the circular trajectory is inherently easier and it permits the simplified control implementation with $\dot{\beta}_{di} := 0$ simultaneously preserving the asymptotic convergence of errors in (6). It is confirmed by bottom plots in Fig. 5 where the last-trailer posture errors converge toward zero and all the joint angles β_i converge to the constant steady-state values β_{is} resulting from the formula $|\beta_{is}| = \frac{\pi}{2} - \arctan(r_i/L_i)$, where $r_i^2 = r_t^2 + L_N^2 + \ldots + L_{i+1}^2$ and $r_t = |v_{tN}/\omega_{tN}| > 0$ is a radius of the reference circle trajectory.

For simulation Sim1 the feed-forward terms $\dot{\beta}_{di}$ have been approximated by their filtered versions $\dot{\beta}_{diF}$ in order to obtain better tracking precision for time-varying reference signals. However, due to the approximations the error convergence obtained in (6) is only the *practical* one with the values of δ_1 and δ_2 depending on the quality of these approximations. This is visible in Fig. 5 where the last-trailer posture errors converge to some small envelope near zero. Influence

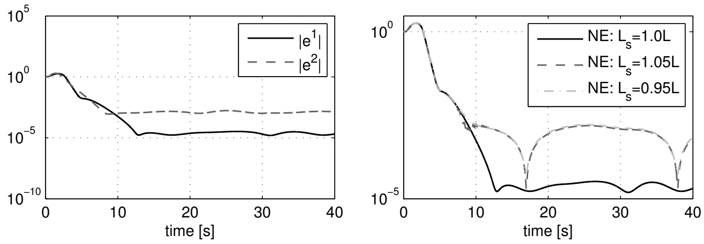

Figure 6: Left: evolution of $\|\,\overline{\mathbf{e}}(\tau)\|$ for two control implementations in Sim1: with the terms $\dot{\beta}_{d1,2,3}$ approximated numerically (denoted by $|e^1|$), and with $\dot{\beta}_{d2,3} := 0$ (denoted by $|e^2|$). Right: closed-loop robustness to parametric uncertainty as a plot of $\|\,\overline{\mathbf{e}}(\tau)\|$ for three sets of vehicle segment lengths: $L_{is} = L_i$ (nominal), $L_{is} = 1.05L_i$ (overestimated), and $L_{is} = 0.95L_i$ (underestimated).

of the quality of numerical approximations for $\dot{\beta}_{di}$ terms is shown in Fig. 6 (left plot) where the evolution of $\|\,\overline{\mathbf{e}}(\tau)\|$ is presented for two scenarios of simulation Sim1: when all the terms $\dot{\beta}_{di}$ are approximated by $\dot{\beta}_{diF}$, and when $\dot{\beta}_{d1}$ is still approximated but $\dot{\beta}_{d2,3}$ are taken as equal to zero (simplified implementation as for Sim2). One can see that in both scenarios stability of the closed-loop system is preserved, but the obtained size of envelope δ_1 is bigger for the simplified control implementation.

In practice the nominal values of parameters L_i used in the recurrence (7) (or (23)) and (8) may be unknown. Robustness of the proposed controller to the parametric uncertainty has been examined by running additional tests for conditions of simulation Sim1 assuming now 5% uncertainty of the vehicle segment lengths. In the first scenario we have used the overestimated parameters by taking in the controller equations the lengths $L_{is} = 1.05 \cdot L_i$. In the second scenario the underestimated parameters $L_{is} = 0.95 \cdot L_i$ have been used. Robustness can be assessed analyzing the right-hand side plots presented in Fig. 6. For the two scenarios stability of the closed-loop system has been preserved. Note that the transient states obtained are virtually indistinguishable in comparison to the nominal case (i.e. when $L_{is} = L_i$).

The control performance obtained in the presence of feedback measurement noises and small offset errors of the trailer hitching points location can be assessed analyzing the preliminary results in Fig. 7. In this case the 0.01 m hitching offsets have been applied to the robot, and the normally distributed measurement noises with variances $V_{\beta 1,2,3} = 10^{-7}$, $V_{\theta,x,y} = 10^{-6}$ have been added to the feedback signals. During the test the simplified control implementation with $\dot{\beta}_{d2,3} := 0$ was used. Note that sensitivity to the measurement noises increases along the vehicle kinematic chain and is the highest on the tractor side.

5 Final remarks

In the paper the novel tracking control strategy for the standard N-trailer robot has been presented. Origins of the concept come from geometrical interpretations of the vehicle kinematics formulated in a cascaded form, and also from propagation of velocities along the vehicle kinematic

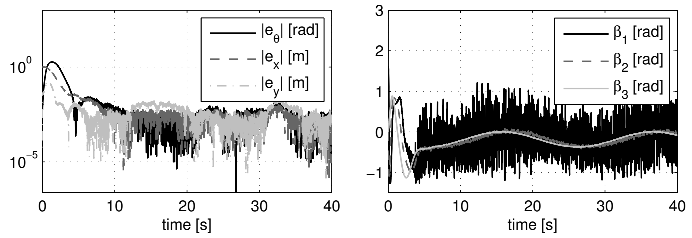

Figure 7: Time plots of the last-trailer posture errors (left) and the joint angles (right) for tracking with small hitching offsets in the vehicle and the measurement noises present in feedback.

chain. The resultant control system consists of two main components: the serial chain of Single Control Modules with the inner joint-angle feedback loops, and the Last-Trailer Posture Tracker in an outer loop dedicated to the last-trailer segment treated as the unicycle.

The question which naturally arises here concerns the possibility of applying in the LTPT block the feedback controllers other than the VFO one proposed above. Preliminary simulation results obtained by the author (however not presented in this paper) indicate that it my be successful. The necessary and sufficient conditions which the outer-loop controllers should meet to ensure stability and convergence of the closed-loop system has to be investigated yet.

Stability of the proposed closed-loop system remains to be shown. The preliminary analysis conducted so far seems to be promising, since it reveals that the dynamics of the last-trailer posture error (5) and the auxiliary joint error $\boldsymbol{e}_d = [e_{d1} \ \dots \ e_{dN}]^T$ can be written as $\dot{\overline{\boldsymbol{e}}} = \boldsymbol{f}(\overline{\boldsymbol{e}}, \tau) + \boldsymbol{f}_1(\overline{\boldsymbol{e}}, \boldsymbol{e}_d, \tau)$ and $\dot{\boldsymbol{e}}_d = \boldsymbol{A}\boldsymbol{e}_d + \boldsymbol{f}_2(\overline{\boldsymbol{e}}, \boldsymbol{e}_d, \tau)$, where $\boldsymbol{f}_1(\overline{\boldsymbol{e}}, \boldsymbol{e}_d, \tau) = \boldsymbol{G}(\overline{\boldsymbol{q}}_t(\tau) - \overline{\boldsymbol{e}})\boldsymbol{\Gamma}\boldsymbol{e}_{\omega v}(\overline{\boldsymbol{e}}, \boldsymbol{e}_d, \tau)$, $\boldsymbol{G}(\cdot)$ is the unicycle kinematics matrix, $\boldsymbol{f}_2(\overline{\boldsymbol{e}}, \boldsymbol{e}_d, \tau) = \boldsymbol{H}\boldsymbol{e}_{\omega v}(\overline{\boldsymbol{e}}, \boldsymbol{e}_d, \tau)$, $\boldsymbol{e}_{\omega v} = [\boldsymbol{e}_\omega^T \ \boldsymbol{e}_v^T]^T$, $\boldsymbol{e}_\omega = [\omega_{d1} - \omega_1 \ \dots \ \omega_{dN} - \omega_N]^T$, $\boldsymbol{e}_v = [v_{d1} - v_1 \ \dots \ v_{dN} - v_N]^T$, $\boldsymbol{A} = \mathrm{diag}\{-k_i\}$ is Hurwitz, and $\boldsymbol{\Gamma}$ and $\boldsymbol{H}$ are the appropriate constant matrices with -1, 0, and $+1$ entries. Furthermore, one can show that $\boldsymbol{f}_2(\boldsymbol{e}_d = \boldsymbol{0}, \cdot) = \boldsymbol{0}$, $\boldsymbol{f}_1(\boldsymbol{e}_d = \boldsymbol{0}, \cdot) = \boldsymbol{0}$, and the nominal (unperturbed) dynamics $\dot{\overline{\boldsymbol{e}}} = \boldsymbol{f}(\overline{\boldsymbol{e}}, \tau)$ is asymptotically stable (see the proof in [4]). We plan to proceed our further analysis using the stability theorems of interconnected systems, [6], showing first the required features of functions $\boldsymbol{f}_1(\cdot)$ and $\boldsymbol{f}_2(\cdot)$. If the convergence for $\overline{\boldsymbol{e}}$ and $\boldsymbol{e}_d$ is shown, the convergence of the joint angle error (4) might result from the flatness property of the vehicle and feasibility of the reference trajectory $\boldsymbol{q}_t(\tau)$. Specifically, since $\Phi_v(\overline{\boldsymbol{e}} = \boldsymbol{0}, \cdot) = v_{tN}(\tau)$ and $\Phi_\omega(\overline{\boldsymbol{e}} = \boldsymbol{0}, \cdot) = \omega_{tN}(\tau)$, then according to (14)-(21) it could be shown that $(\beta_{di} - \beta_{ti}) \to 0$ as $\overline{\boldsymbol{e}} \to \boldsymbol{0}$, which would complete the proof recalling the asymptotic convergence of $\boldsymbol{e}_d$.

Acknowledgement This work was supported by the Polish scientific fund in years 2010-2012 as the research project No. N N514 087038.

References

[1] N. P. I. Aneke, H. Nijmeijer, and A. G. de Jager. Tracking control of second-order chained from systems by cascaded backstepping. *Int. J. Robust Nonlinear Control*, 13:95–115, 2003.

[2] F. Bullo and R. M. Murray. Experimental comparison of trajectory trackers for a car with trailers. In *IFAC World Congress*, pages 407–412, 1996.

[3] A. De Luca and G. Oriolo. Local incremental planning for nonholonomic mobile robots. In *IEEE Int. Conf. on Robotics and Automation*, pages 104–110, 1994.

[4] M. Michałek and K. Kozłowski. Vector-Field-Orientation feedback control method for a differentially driven vehicle. *IEEE Trans. on Control Syst. Technology*, 18(1):45–65, 2010.

[5] F. Jean. The car with N trailers: characterisation of the singular configurations. *Control, Opt. Calc. Variations*, 1:241–266, 1996.

[6] H. K. Khalil. *Nonlinear systems. 3rd Edition.* Prentice-Hall, New Jersey, 2002.

[7] D. Kim and J. Oh. Globally asymptotically stable tracking control for a trailer system. *Journal of Robotic Systems*, 19(5):199–205, 2002.

[8] J. P. Laumond. Controllability of a multibody mobile robot. *IEEE Transactions on Robotics and Automation*, 9(6):755–763, 1993.

[9] A. Levant. Higher-order sliding modes, differentiation and output-feedback control. *Int. J. Control*, 76(9/10):924–941, 2003.

[10] P. Morin and C. Samson. Transverse function control of a class of non-invariant driftless systems. Application to vehicles with trailers. In *Proceedings of the 47th IEEE Conference on Decision and Control*, pages 4312–4319, Cancun, Mexico, 2008.

[11] C. Pradalier and K. Usher. Robust trajectory tracking for a reversing tractor trailer. *Journal of Field Robotics*, 25(6-7):378–399, 2008.

[12] O. J. Sørdalen. Conversion of the kinematics of a car with n trailers into a chained form. In *Proc. IEEE Int. Conf. on Robotics and Automation*, pages 382–387, Atlanta, USA, 1993.

[13] P. Rouchon, M. Fliess, J. Levine, and P. Martin. Flatness, motion planning and trailer systems. In *Proceedings of the 32nd Conference on Decision and Control*, pages 2700–2705, San Antonio, Texas, 1993.

[14] O.J. Sørdalen and O. Egeland. Exponential stabilization of nonholonomic chained systems. *IEEE Transactions on Automatic Control*, 40(1):35–49, 1995.

[15] D. Zöbel. Trajectory segmentation for the autonomous control of backward motion for truck and trailer. *IEEE Trans. Intell. Transportation Systems*, 4(2):59–66, 2003.